Ali, Abdelfatah; Mahmoud, Karar; Raisz, David; Lehtonen, Matti

Optimal Allocation of Inverter-Based WTGS Complying with their DSTATCOM Functionality and PEV Requirements

Published in:
IEEE Transactions on Vehicular Technology

DOI:
10.1109/TVT.2020.2980971

Published: 01/01/2020

Document Version
Peer reviewed version

Please cite the original version:
Ali, A., Mahmoud, K., Raisz, D., & Lehtonen, M. (2020). Optimal Allocation of Inverter-Based WTGS Complying with their DSTATCOM Functionality and PEV Requirements. *IEEE Transactions on Vehicular Technology*, *69*(5), 4763-4772. [9036991]. https://doi.org/10.1109/TVT.2020.2980971

Optimal Allocation of Inverter-Based WTGS Complying with their DSTATCOM Functionality and PEV Requirements

Abdelfatah Ali, Karar Mahmoud, David Raisz, *Senior Member, IEEE*, and Matti Lehtonen

***Abstract*— Recently, the integration of inverter-based wind turbine generation systems (WTGS) and plug-in electric vehicles (PEV) has remarkably been expanded into distribution systems throughout the world. These distributed resources could have various technical benefits to the grid. However, they are also associated with potential operation problems due to their stochastic nature, such as high power losses and voltage deviations. An optimization-based approach is introduced in this paper to properly allocate multiple WTGS in distribution systems in the presence of PEVs. The proposed approach considers 1) uncertainty models of WTGS, PEV, and loads, 2) DSTATCOM functionality of WTGS, and 3) various system constraints. Besides, the realistic operational requirements of PEVs are addressed, including initial and preset conditions of their state of charge (SOC), arriving and departing times, and various controlled/uncontrolled charging schemes. The WTGS planning paradigm is established as a bi-level optimization problem which guarantees the optimal integration of multiple WTGS, besides optimized PEV charging in a simultaneous manner. For this purpose, a bi-level metaheuristic algorithm is developed for solving the planning model. Intensive simulations and comparisons with various approaches on the 69-bus distribution system interconnected with four PEV charging stations are deeply presented considering annual datasets. The results reveal the effectiveness of the proposed approach.**

***Index Terms*—Distribution systems, PEV charging; energy losses; system constraints; WTGS allocation.**

I. Introduction

RENEWABLE energy sources (RESs) are growing year by year throughout the world. Since greenhouse-gas emissions are highly problematic, breakthroughs are required for the future forms of electrical energy productions. Indeed, inverter-based wind turbine generation systems (WTGS) can be considered one of the most promising categories of RESs. Such distributed units along the feeders of medium voltage (MV) distribution systems could have pronounced positive impacts on the consumers, and especially utilities. Specifically, WTGS with their DSTATCOM control functionalities could increase the supply reliability rate, regulate voltage, mitigate power quality issues, reduce the stress over the traditional voltage control devices, and reduce power losses [1]–[3]. However, the uncertainty feature of WTGS profiles could cause considerable technical and operational consequences, thereby limiting their maximum allowed hosting capacities.

In conjunction with the great interest in WTGS, the penetration of plug-in electric vehicles (PEVs) has widely been growing throughout the world [4]–[6]. A multi-government policy forum labeled 'Electric Vehicle Initiative' was dedicated to accelerating the introduction of electric vehicles where their number is aimed to be raised to 20 million within 2020 [7]. From the perspective of utility, PEVs are considered electric-based units involving storage capability to be employed during the parking time while fulfilling their charging target [8]–[10]. It is a statistical fact that the typical parking period of PEVs is higher than ninety percent of the day [11], and so their energy storage capability can be managed by the aggregators [12]. Nevertheless, they could cause line congestions and voltage violations in distribution systems if uncontrolled schemes are utilized [13].

Several methods and studies have been performed on the optimal allocation of WTGS while highlighting their positive impacts on MV distribution systems. In [14], a probabilistic planning model of RESs including WTGS with unity power factors is presented to minimize energy losses and fulfill operational constraints. Analytic methods have been introduced in [15]–[17] for the optimal sizing and placement of WTGS with considering the rated condition of the distribution system, i.e. ignoring their intermittent nature. A multi-objective probabilistic framework for planning WTGS and other RES types has been proposed in [18] for reducing costs and emissions whereas an augmented ε-constraint equipped with fuzzy roles have been utilized. In [19]–[21], a

Project no. FIEK_16-1-2016-007 has been implemented with the support provided from the National Research, Development and Innovation Fund of Hungary, financed under the FIEK_16 funding scheme.

A. Ali is with the Faculty of Engineering, South Valley University, 83523 Qena, Egypt, and also with the Faculty of Electrical Engineering and Informatics, Budapest University of Technology and Economics, 1111 Budapest, Hungary (e-mail: abdelfatah.mohamed@vet.bme.hu).

K. Mahmoud is with the Department of Electrical Engineering and Automation, Aalto University, FI-00076 Espoo, Finland, and also with the Faculty of Engineering, Aswan University, 81542 Aswan, Egypt (e-mail: karar.alnagar@aswu.edu.eg).

D. Raisz is with the Faculty of Electrical Engineering and Informatics, Budapest University of Technology and Economics, 1111 Budapest, Hungary (e-mail: raisz.david@vet.bme.hu).

M. Lehtonen is with the Department of Electrical Engineering and Automation, Aalto University, FI-00076 Espoo, Finland (email: matti.lehtonen@aalto.fi).

hydro-turbine governing system with actuator failures and disturbance have been investigated. Driven by the recent innovations in metaheuristic based optimizers, several variants are applied to solve the RES planning problem, such as ant colony optimizer [22], genetic-based methods [23], simulated annealing [24], and tabu search algorithm [25]. Authors of [12] have emphasized the essential role of flexible energy storage systems, especially PEVs, to expand the penetration of various RESs in the distribution system. In [26], various fleets of PEV have been controlled by smart strategies to investigate their contribution to increasing RES penetration.

As illustrated above, considerable methods and studies have focused on the optimal WTGS allocation in power distribution systems. Nevertheless, to reduce the computational complexity of the WTGS planning model, various existing approaches assume a single allocation of WTGS without considering their DSTATCOM functionalities while utilizing deterministic models instead of the probabilistic ones. Most importantly, many of these approaches ignore the intermittent and uncertain nature of PEVs or even ignore their presence. Indeed, these fast-growing mobile energy storage devices play a vital role in current/future distribution systems, and so their impact on WTGS planning is significant. For this purpose, detailed PEVs modeling complying with their charging requirement is necessary, including the control schemes of PEVs and their various stochastic variables. To fill the gap in the literature, this work has been directed to this vital recent research topic, where further investigations and developments are required in distribution systems with PEVs and WTGS.

An optimization-based approach is proposed in this work to accurately allocate multiple WTGS for maximizing annual energy loss reductions. It is worth mentioning that the location of WTGS is determined by windy locations, rather than the requirements of the power system. However, in the distribution systems, the wind speeds at all locations are almost the same. Therefore, determining the optimal locations of WTGS is considered in this work. The proposed approach considers DSTATCOM functionalities of the interfacing inverter of WTGS and complying with existing PEV infrastructures. The comprehensive planning model incorporates the uncertainty of WTGS generation and load demand, and the various operational limits of the distribution system, the allocated WTGS units, and PEVs. To accurately solve the comprehensive optimization model, a bi-level gray wolf optimization (GWO) algorithm is introduced in which the upper level guarantees an optimal allocation of multiple WTGS while the lower level optimizes PEV charging in a simultaneous manner. The effect of the PEV charging scheme on the optimal calculated results of WTGS (in terms of locations and capacities) are investigated and verified. Furthermore, various comparisons with existing approaches are introduced, and the effect of the inverter oversizing in WTGS is studied.

II. Formulation of the Allocation Problem

A. Objective function

In this work, the optimal allocation of inverter-based WTGS is aimed to be computed in the presence of PEVs. Two uncertain parameters are considered in the optimization problem which are load demand and power generation by WTGS. The annual energy losses in the distribution system for all possible combination of the uncertain parameters in the presence of PEVs is utilized as an objective function to be minimized. At each time segment, which denotes $\Delta\tau$ hours, the probability distribution function (pdf) of the uncertain parameters are divided into numerous states. The energy losses must be computed and then weighted based on the occurrence probability of each individual state in the whole planning period. The mathematical formulation of the objective function is written as follows:

$$Minimize \quad f = \sum_{t=1}^{n_t}\sum_{s=1}^{n_s} E^t_{loss,s} \times P^t_{com}(\lambda_s) \tag{1}$$

in which

$$E^t_{loss,s} = P^t_{loss,s} \times \Delta\tau, \qquad \forall s,\tau \tag{2}$$

where $E^t_{loss,s}$ and $P^t_{com}(\lambda_s)$ are the total energy losses and the combined probability set of wind speed and load demand, respectively; λ_s is a two columns matrix which includes all possible combinations of the states of power generation by WTGS and the load states; n_t and n_s denotes, the numbers of time segments and states, respectively.

The next constraints are considered in the optimization problem

$$P^t_{G,1,s} + \lambda(s,1)P^t_{WTGS,i} - \lambda(s,2)P^t_{d,i} \pm P^t_{CS,i,s} - V^t_{i,s}\sum_{j=1}^{n_b} V^t_{j,s}\left[G_{ij}\cos\delta^t_{ij,s} + B_{ij}\sin\delta^t_{ij,s}\right] = 0, \forall i \notin \phi_b, s, t \tag{3}$$

$$Q^t_{G,1,s} \pm Q^t_{inv,i,s} - \lambda(s,2)Q^t_{d,i} - V^t_{i,s}\sum_{j=1}^{n_b} V^t_{j,s}\begin{bmatrix} G_{ij}\sin\delta^t_{ij,s} \\ +B_{ij}\cos\delta^t_{ij,s}\end{bmatrix} = 0, \forall i \notin \phi_b, s, t \tag{4}$$

$$V^t_{1,s} = 1.0, \quad \delta^t_{1,s} = 0.0 \tag{5}$$

$$V^{min} \le V^t_{i,s} \le V^{max}, \qquad \forall i \in \phi_b, s, t \tag{6}$$

$$P^{min,t}_{cs,i,s} \le P^t_{CS,i,s} \le P^{max,t}_{cs,i,s}, \qquad \forall i \in \phi_b, s, t \tag{7}$$

$$P^{min}_{WTGS,i} \le P_{WTGS,i} \le P^{max}_{WTGS,i}, \qquad \forall i \in \phi_b \tag{8}$$

$$Q^{min,t}_{inv,i,s} \le Q^t_{inv,i,s} \le Q^{max,t}_{inv,i,s}, \qquad \forall i \in \phi_b, s, t \tag{9}$$

$$\sum_{i=1}^{N_{WTGS}} P_{WTGS,i} \le \sum_{i=1}^{N_l} P^t_{d,i,s} + P^t_{loss,s}, \qquad \forall i \in \phi_b, s, t \tag{10}$$

$$SOC_{n,d,s} \ge SOC_{n,min,s} \tag{11}$$

where B_{ij} and G_{ij}, are the susceptance and conductance of line ij, respectively; $V^t_{i,s}$, and $\delta^t_{ij,s}$ are the magnitude of voltage at node i, and the variance of the voltage angles at nodes i and j, respectively; $P^t_{G,1,s}, P^t_{WTGS,i,s}, P^t_{d,s}$, and $P^t_{CS,j,s}$ are the grid active power, WTGS power generation, load demand and power of the charging station, respectively; n_b, n_{WTGS}, and n_l represent, respectively, the number of nodes, WTGS number, and number of loads,; $Q^t_{G,1,s}$ and $Q^t_{d,i}$ are the reactive power of the main distribution substation and reactive power demand, respectively. $P^{min,t}_{cs,i,s}$ and $P^{max,t}_{cs,i,s}$ represent, respectively, the lowest and highest allowed active power of the charging station at bus i; $P^{min}_{WTGS,i}$ and $P^{max}_{WTGS,i}$ represent, respectively, the lowest and highest allowed power of WTGS at bus i, respectively;

$Q^t_{inv,i,s}$ is the inverter reactive power at i; $Q^{max}_{inv,i,s}$ and $Q^{min}_{inv,i,s}$ are the maximum and minimum reactive power of the inverter at bus i, respectively; V^{min} and V^{max} represent the upper and lower voltage boundaries, respectively. $V^t_{1,s}$ and $\delta^t_{1,s}$ represent, respectively, the voltage magnitude and the corresponding angle at the slack bus (bus 1). ϕ_b denotes a set of the system nodes. $SOC_{n,d,g}$ represents the value of the state of charge (SOC) for n^{th} battery at parting instant, and $SOC_{n,min,g}$ is the lowest SOC selected by the corresponding vehicle owner, respectively. In this work, WTGS is defined as a wind farm, which contains multiple wind turbine (WT) units at a certain bus.

B. PEV battery Model

The main characteristic of the battery of PEV is its SOC. SOC is defined as the percentage of remained energy in a battery with respect to its total capacity. Based on the charging/discharging status of every PEV battery, its SOC at each time instant t is updated according to the following:

$$SOC^t_{n,s} = SOC^{t-1}_{n,s} + \eta_{ch,n} P^t_{ch,n,s} \Delta t \delta - \Delta t \gamma P^t_{dc,n,s} / \eta_{dc,n} \quad (12)$$

where $P^t_{ch,n,s}$ and $P^t_{dc,n,s}$ represent, respectively, the charging and discharging powers of n^{th} PEV battery; δ and $\gamma \in \{0,1\}$, in which δ. $\gamma = 0$ because the PEV battery cannot charge and discharge simultaneously. $\eta_{ch,n}$, and $\eta_{dc,n}$ are the charging and discharging efficiencies of n^{th} PEV, respectively.

The charging/discharging power of each PEV represents a part of the total charging or discharging power of the PEV station. This part of the power affected by the capacity of the PEV battery ($C_{batt,n}$), its SOC ($SOC^t_{n,s}$), its arrival time (T_{arr}), and its departure times ($T_{d,n}$). The charging/discharging power of n^{th} PEV is formulated as follows:

$$P^t_{ch,n,s} = \frac{\left(C_{batt,n} - SOC^t_{n,s} \times C_{batt,n}\right) \times P^t_{CS,s}}{T_{rem,n} \times \sum_{j=1}^{m} \frac{1}{T_{rem,j}} \left(C_{batt,j} - SOC^t_{j,s} \times C_{batt,j}\right)} \quad (13)$$

$$P^t_{dc,n,s} = \frac{T_{rem,n} \left(SOC^t_{n,s} \times C_{batt,n}\right) \times P^t_{CS,s}}{\sum_{j=1}^{m} T_{rem,j} \left(SOC^t_{j,s} \times C_{batt,j}\right)} \quad (14)$$

in which

$$T_{rem,n} = T_{d,n} - T_{arr,n} \quad (15)$$

The aggregator of PEVs divides the charging station active power which is computed via the optimization algorithm among the PEVs using (13)-(15) according to their present SOC and their departure time. Note that some PEVs have DSTATCOM functionality. However, the utilized PEV charger is considered to work at a unity power factor, and so this functionality is not enabled in this work.

C. Stochastic Behavior of PEV

The profile of PEVs contains many stochastic variables. These stochastic variables include the arrival time to the home from the last trip, daily milage, departure time, and driving habits. Furthermore, the total capacity and efficiency of the PEV batteries. Because of the stochastic nature of PEVs usage, they do not connect to the grid at the same time. Hence, all these stochastic variables should be taken into account since they are key characteristics that can define PEV owners' behavior and preferences.

In this work, we assume that each PEV is charged/ discharged only at the charging station. The arrival time of each PEV is a random variable with a normal probability density function (pdf) [27]. The daily arrival time pdf of PEV battery can be computed as follows:

$$f^t_n(T_{arr}) = \exp\left[-(T_{arr} - \mu^t_{T_{arr}})^2 / 2(\sigma^t_{T_{arr}})^2\right] \Big/ (\sigma^t_{T_{arr}} \sqrt{2\pi}) \quad (16)$$

where $\mu^t_{T_{arr}}$ and $\sigma^t_{T_{arr}}$ are the mean and standard deviation of daily arrival time and they are 18 and 5 hours, respectively.

The initial SOC of a PEV battery depends on daily mileage (dm_n), all-electric range (AER_n), and SOC of the battery at the preceding parting time (it is assumed to be 100%). To protect the PEV batteries against degradation, the depth of discharge (DOD) should not be more than 80% (i.e. the SOC should not be less than 20%). Hence, the initial value of SOC for a PEV battery can be calculated by:

$$SOC_{initial,n}(\%) = \begin{cases} (1 - dm_n / AER_n) \times 100, & 0 < dm_n < 0.8 AER_n \\ 20\%, & dm_n > 0.8 AER_n \end{cases} \quad (17)$$

$$AER = C_{batt,n} / E_{cons/mile,n} \quad (18)$$

where $C_{batt,n,}$ and $E_{cons/mile,n}$ are the capacity of the n^{th} PEV battery and energy consumption per mile, respectively. The randomness of the PEV daily mileage can be represented using a lognormal pdf, considering the probability occurrence of negative distances is zero, and a tail extending to infinity for positive distance [27]. The pdf of PEV daily mileage can be expressed as follow:

$$f^t_n(dm) = \frac{1}{dm_n \sqrt{2\pi (\sigma^t_{dm,n})^2}} \times \exp\left[\frac{-(\ln dm_n - \mu^t_{dm,n})^2}{2(\sigma^t_{dm,n})^2}\right], \; dm_n > 0 \quad (19)$$

where μ^t_{dm} and σ^t_{dm} are the mean and standard deviation of daily mileage and they are 22.3 and 12.3 miles, respectively.

It is a fact that the historical/expected conditions that are considered in the planning phase can be not totally matched with the actual future situations, but this is a general trend in planning science. To deal with this issue in this paper, it is important to mention that the utilization of the probability model of PEVs (not a deterministic model) can represent their stochastic nature. Therefore, for any distribution system, it is required to gather full data of PEVs (i.e. including initial and preset conditions of their SOC, arriving and departing times, and various controlled/uncontrolled charging schemes) to construct the probabilistic model to be used in the planning phase.

III. Modeling Wind Speed and Load

Here, the stochastic behaviors of the output power by wind turbine and load demand are described. Weibull pdf and normal pdf are utilized to model hourly wind speed and hourly load demand, respectively [28]–[30].

A. Hourly Wind Speed Modeling

To model the hourly stochastic nature of wind speed and output power by WTGS, Weibull pdf is commonly used for

this purpose. The Weibull pdf (f_W) at time segment t of the wind speed v can be determined as follows:

$$f_W^t(v) = k/c\left(v/c\right)^{k-1} \exp\left[-\left(v/c\right)^k\right] \quad (20)$$

where c and k are the scale parameter and shape parameter, respectively. There are different methods that can be used to determine these parameters (c and k) [31], [32]. In this work, the Weibull parameters are calculated using the mean (μ_v) and the standard deviation (σ_v) of the wind speed as follows:

$$k = \left(\sigma_v/\mu_v\right)^{-1.086} \quad (21)$$

$$c = \mu_v/\Gamma(1+(1/k)) \quad (22)$$

The probability of wind speed for each state can be computed as follows:

$$P_v^t(G_w) = \int_{v_{w1}}^{v_{w2}} f_W^t(v).dv \quad (23)$$

where $P_v^t(G_w)$ is the wind speed probability in state w; v_{S1} and v_{S2} are the wind speed limits of state s

The power generated by each WT of the WTGS for each state can be determined by using the characteristics of WT and the average value of the wind speed at this state as follows:

$$P_{WT_w}^t = \begin{cases} 0, & 0 \le v_{avw} < v_{ci} \\ P_{rated} \times (v_{av} - v_{ci})/(v_r - v_{ci}), & v_{ci} \le v_{avw} < v_r \\ P_{rated}, & v_r \le v_{avw} < v_{co} \\ 0, & v_{avw} \ge v_{co} \end{cases} \quad (24)$$

where v_{ci}, v_{co}, and v_r are cut-in speed, cut-off speed and rated speed of the WT, respectively; v_{avw} and P_{rated} are the average wind speed at state w and rated power of the WT, respectively; $P_{WT_w}^t$ is the output power of WT during state w of time segment t. It worth mentioning that we have used the linear not the cubic relation since it is widely used for planning purposes [14], [29], [33]. In this work, WT with a rated power of 200 kW, cut-in speed of 2.5 m/s, rated speed of 11.5 m/s, and cut-off speed of 20 m/s is used [34].

B. Hourly Load Demand Modeling

Because of the stochastic behavior of consumers, the load demand in the distribution system will be uncertain. To model this uncertainty of load demand, a normal pdf is used for this purpose. The pdf of the load demand can be defined by a mean (μ_l) and standard deviation (σ_l at time segment t as follows:

$$f_l^t(l) = \exp\left[-(l-\mu_l^t)^2/2(\sigma_l^t)^2\right]\Big/(\sigma_l^t\sqrt{2\pi}) \quad (25)$$

The probability of the load demand for state u of time segment t is calculated by:

$$P_l^t(G_u) = \int_{l_{u1}}^{l_{u2}} f_l^t(v).dv \quad (26)$$

where $P_l^t(G_s)$ is the load demand probability in state u; l_{u1} and l_{u2} represent the load limits of state u.

C. Combined Wind-load pdf Model

The probability models of wind speed and load demand are used for generating a combined wind-load model. The combined probability can be computed by convolving the wind speed and load probabilities, as follows:

$$P_{com}^t(\lambda_s) = P_v^t(G_w) \times P_l^t(G_u) \quad (27)$$

The complete wind–load model is calculated by listing the possible combinations of wind power and the load. Hence, the Wind–load model is calculated by using the flowing formula:

$$\phi = \left[\{\lambda_s, P_{com}(\lambda_s)\} : s = 1 : n_s\right] \quad (28)$$

where ϕ is the complete Wind-load model; $P_{com}(\lambda_s)$ includes the combined probability with respect to the matrix λ. It is important to note that the proposed model can consider other factors, such as solar PV generations and battery energy storage systems in distribution systems. To do so, these units will be treated as negative loads, and so the probabilistic model of the net loading in the distribution system will be built. However, we have not dealt with these factors in this work.

IV. Gray Wolf Optimization (GWO)

GWO is a population-based metaheuristic method that has been proposed in [35] by Mirjalili et al. The GWO method simulates the leadership hierarchy and hunting mechanism of grey wolves in nature. The leadership hierarchy is defined as alpha (α) for the best wolf, beta (β) for the second-best one, delta (δ) for the third-best one, and omega (ω) for all other individuals.

During the hunting process, gray wolves encircle the prey at first. Encircling behavior is mathematically formulated by:

$$\vec{D} = |\vec{C}.\vec{X}_p(iter) - \vec{X}(iter)| \quad (29)$$

$$\vec{X}(iter+1) = \vec{X}_p(iter) - \vec{A}.\vec{D} \quad (30)$$

where *iter* is the present iteration; A and C represent coefficient vectors; X_p, X, and D are the position vector of the prey, position vector of the grey wolf, and distance from prey location, respectively.

The coefficient vectors (A and C) can be computed by:

$$\vec{A} = 2\vec{a}.\vec{r}_1 - \vec{a} \quad (31)$$

$$\vec{C} = 2.\vec{r}_2 \quad (32)$$

where the components of a decreased linearly from two to zero over the iterations, and they are used to coordinate the exploration and exploitation ability; r_1 and r_2 represent random vectors.

The hunting process is usually guided by α and called leaders followed by β and δ. Nevertheless, the location of the prey is unidentified in the abstract search space. To imitate the hunting behavior, α (best solution), β and δ are assumed to have better knowledge about the location of prey. Hence, the three best solutions on the decision level are saved and guide the other search agents to update their positions every iteration. The following formulas can be used in this regard:

$$\vec{D}_\alpha = |\vec{C}_1.\vec{X}_\alpha - \vec{X}|, \vec{D}_\beta = |\vec{C}_2.\vec{X}_\beta - \vec{X}|, \vec{D}_\delta = |\vec{C}_3.\vec{X}_\delta - \vec{X}| \quad (33)$$

$$\vec{X}_1 = \vec{X}_\alpha - \vec{A}_1.\vec{D}_\alpha, \vec{X}_2 = \vec{X}_\beta - \vec{A}_2.\vec{D}_\beta, \vec{X}_3 = \vec{X}_\delta - \vec{A}_3.\vec{D}_\delta \quad (34)$$

$$\vec{X}(iter+1) = (\vec{X}_1 + \vec{X}_2 + \vec{X}_3)\Big/3 \quad (35)$$

The GWO algorithm has merit in terms of the exploration phase, and so it provides very competitive results compared

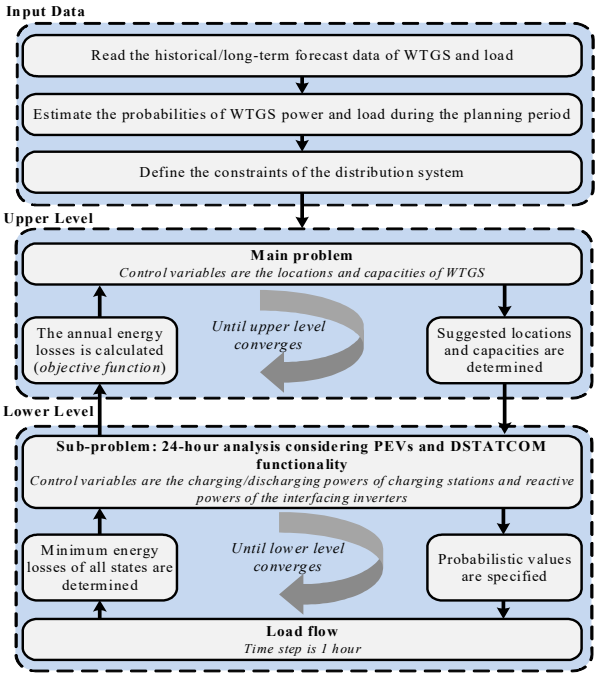

Fig. 1. Solution process for determining the optimal capacities and locations of WTGS.

with well-known meta-heuristic algorithms. Also, it was shown up to be a reliable and robust optimization algorithm that can be applied to the allocation problems of RES [36]. Therefore, it is used in this paper for solving the optimization model.

V. Solution Process

The solution process of the presented approach for deciding the proper capacities and locations of WTGS considering PEVs and DSTATCOM functionality of the interfacing inverters is explained in Fig. 1. As displayed in the figure, the historical/long-term forecast data of WTGS and load are read, and the corresponding probabilities are generated. Furthermore, all constraints of the distribution system are defined. Then, the optimal planning of the WTGS considering PEVs and DSTATCOM functionality of the inverter is deemed as a bi-level optimization problem and is solved by utilizing GWO. The main problem and sub-problem are solved at the upper level and lower level, respectively.

The optimal capacities and locations of WTGS for the planning period should be determined in the upper level. For this purpose, the optimal charging/discharging power of the charging stations and the optimal injecting/absorbing reactive power of the interfacing inverter should be considered. The optimal scheduling of PEVs and the optimal reactive power of the interfacing inverters can be solved in the lower level as a sub-routine of the planning model. Therefore, the outputs of the lower level are the probabilistic optimal profiles of the charging/discharging power of PEVs and injecting/absorbing reactive power of the inverters. A load flow is used to determine the objective function during each state. In the next paragraph, the solution process to this combinatorial optimization model is explained.

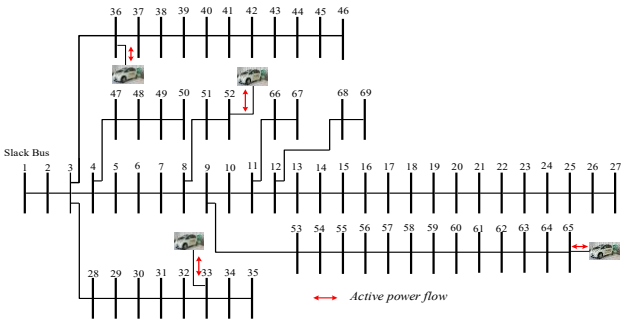

Fig. 2. Single line diagram of the 69-bus radial distribution system.

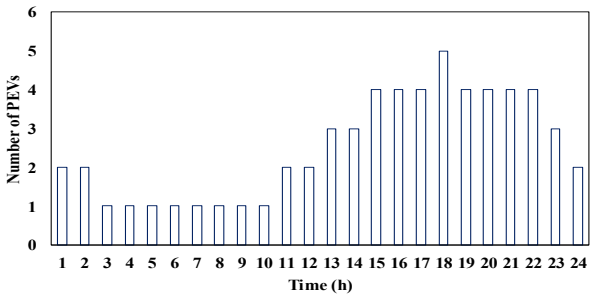

Fig. 3. Hourly distribution of 60 PEVs.

The upper level suggests the optimal capacities and locations of the WTGS. The lower level utilizes these capacities and locations and calculates the energy losses, optimal PEV charging/discharging power, and optimal injecting/absorbing reactive power of the inverters during the day. It is worth mentioning that the WTGS locations and capacities are kept the same during the performing of the lower level. The searching for optimal capacities and locations of the WTGS will not be affected, because the probability of the PEVs is used with each candidate capacity and location. With respect to Fig. 1, the problem is a bi-level optimization problem in which the upper level includes an inner optimization problem as a sub-problem (lower level). Therefore, for each iteration of the upper-level, the lower-level should be entirely executed many times for the corresponding capacities and locations of WTGS. On the other hand, for each iteration of the lower level, the power flow must be executed many times to calculate the optimal PEV power and injecting/absorbing reactive power of the interfacing inverters for every state of time segment *t*. Also, it calculates the value of the respective objective function. The individual objective functions for all time segments and states are collected and utilized as an objective function of the upper level. This process is repeated until the convergence of the upper level.

VI. Results and Discussion

To demonstrate the effectiveness of the proposed approach, the IEEE 69-bus test distribution system is used as a case study as shown in Fig. 2. The complete details of this system can be found in [37]. The base active power, reactive power, and voltage of that system are 3.802 MW, 2.695 Mvar, and 12.66 kV, respectively. A charging station is supposed to be connected at nodes 33, 36, 52, and 65 as illustrated in Fig. 2. Every PEV station is able to accommodate sixty PEVs. The PEV number that is connected to the charging station each hour follows the distribution given in Fig. 3 which was

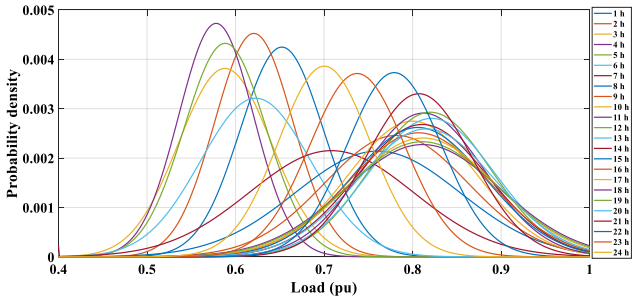

Fig. 4. The pdf of load demand for different time segments.

determined based on (16). The initial SOC of every PEV can be calculated using (17)-(19).

Tesla Model S batteries with 85 kWh capacity are considered for PEVs in this work [38]. Most of PEVs normally back home after the working hours (around 18:00), and they leave in the morning (around 7:00). Therefore, every PEV is supposed to be connected to the distribution system for 12 hours. To guarantee enough SOC of each PEV at its parting time for daily mileages, the vehicle-to-grid technology should consider the constraint provided in (11). The maximum charging/discharging rate of each PEV is $0.2C_{batt,n}$ ($C_{batt,n}$=85 kWh) [39]. On the other hand, the pdf of the load demands each time segment for the whole day is shown in Fig. 4. The proposed approach is performed without and with considering the DSTATCOM functionality of the interfacing inverter of the WTGS. To establish the efficiency of the presented approach, it is assessed for single and multiple locations of WTGS. Three years of historical data for wind speed and load are used to generate their probability. These data are collected from [40] and [41], respectively. The three years are represented by a day throughout these years. The simulations are conducted on MATLAB.

A. WTGS Allocation without DSTATCOM functionality

Here, the proposed approach is tested and compared to the Base case and two different approaches without taking into account the DSTATCOM functionality of the interfacing inverters (i.e. unity power factor of the interfacing inverters). These different approaches are as follows:

Base case: in this case, PEVs start to uncontrollably charge once they are connected to charging stations without WTGS.

Approach 1: the optimal allocation of the WTGS is determined while the uncontrolled charging effect of PEVs is not considered.

Approach 2*:* the optimal WTGS allocation is computed with considering uncontrolled PEV charging.

Approach 3*:* the optimal WTGS allocation is computed by considering optimal PEV charging/discharging (full proposed approach).

TABLE I
RESULTS OF THE APPROACHES WITH 1, 2, AND 3 WTGS

Number of WTGS	Utilized approach	Optimal bus	Number of WT units	Energy losses (MWh)
No WTGS	Base case	-	-	1740
1 WTGS	Approach 1	64	12	822
	Approach 2	62	14	744
	Approach 3	61	14	696
2 WTGS	Approach 1	11	7	741
		64	11	
	Approach 2	12	6	672
		62	13	
	Approach 3	11	7	635
		61	13	
3 WTGS	Approach 1	11	5	715
		17	3	
		64	11	
	Approach 2	12	3	654
		18	3	
		62	13	
	Approach 3	11	4	610
		18	3	
		61	13	

The results of the base case and the three approaches are given in Figs. 5-8 and Table I in which the lines represent the power losses (P_{loss}) while the bars represent the percentage of loss reduction for different approaches. Specifically, Figs. 5, 6, and 7 compare power losses and power loss reduction by the three approaches with 1, 2, and 3 WTGS, respectively. It can be seen from Figs. 5-6 that by applying the different three approaches, the hourly energy losses are significantly reduced compared with the base case. However, considering the PEVs in the planning problems (Approach 2 and Approach 3) leads to a higher reduction in the energy losses compared to Approach 1 in which it does not consider the effect of PEVs. Furthermore, Approach 3 gives the highest reduction in the energy losses compared to other approaches where it considers the effect of PEVs in the planning problem with optimal charging/discharging technique. For instance, as given in Table I, the annual energy losses for Approach 3 are 696 MWh, 635 MWh, and 610 MWh for 1 WTGS, 2 WTGS, and 3 WTGS, respectively, compared to 1740 MWh for the base case. While they are 744 MWh, 672 MWh, and 654 MWh for Approach 2 and 822 MWh, 741 MWh, and 715 MWh for Approach 1 for 1 WTGS, 2 WTGS, and 3 WTGS, respectively. The locations and capacities (number of WT units) of WTGS differ based on the applied approach. Annual energy reduction of different approaches with respect to the base case is shown in Fig. 8. It can be noted from this figure that, for all approaches, with increasing the allocated WTGS number, the annual energy loss reduction is increased. This

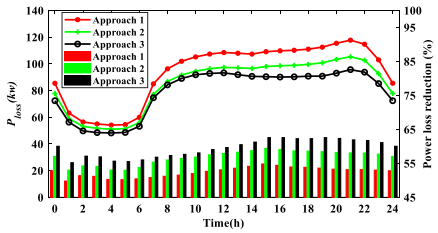

Fig. 5. Hourly active power losses and loss reduction in the distribution system (1 WTGS).

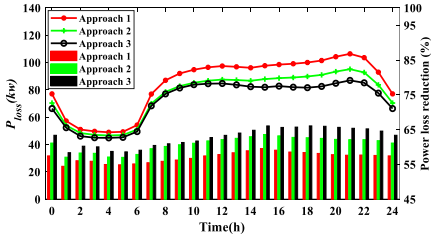

Fig. 6. Hourly active power losses and loss reduction in the distribution system (2 WTGS).

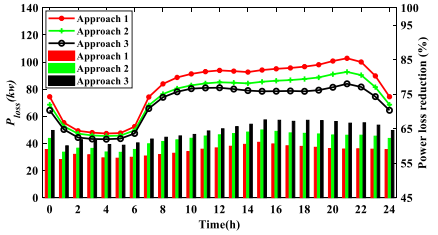

Fig. 7. Hourly active power losses and loss reduction in the distribution system (3 WTGS).

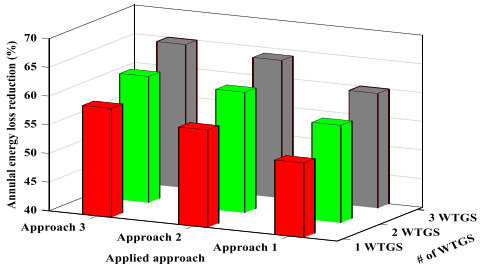

Fig. 8. Annual energy reduction of different approaches compared to the base case.

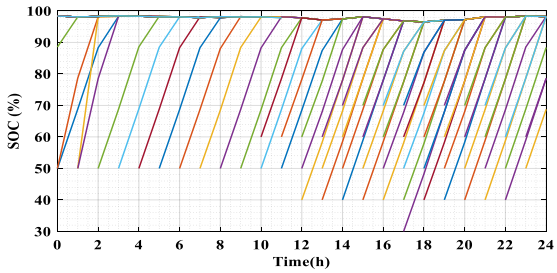

Fig. 9. SOC of PEV batteries with uncontrolled charging scheme (Base case, Approaches 1 and 2).

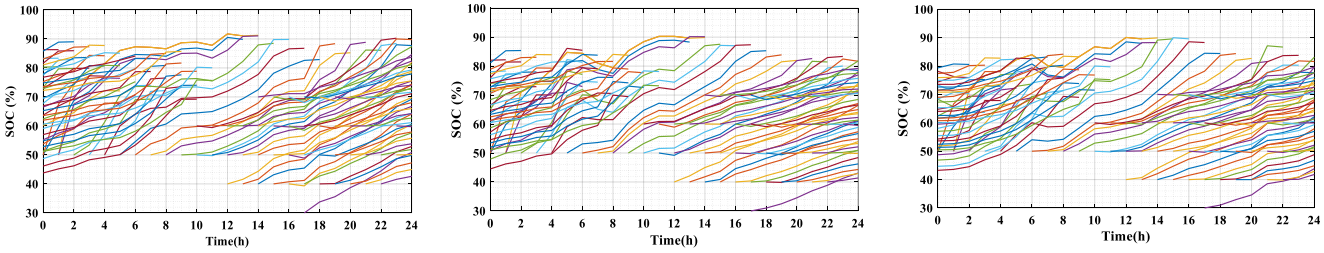

(a) (b) (c)

Fig. 10. SOC of PEV batteries with the optimal charging/discharging scheme for Approach 3. a) 1 WTGS, b) 2 WTGS, and c) 3 WTGS.

implies that the benefits of these renewable units in terms of loss reduction can be increased by distributing such resources to multiple buses instead of a single bus. Further, the annual energy losses are significantly reduced by Approach 3 compared with Approaches 1 and 2 for different WTGS numbers.

The SOC of PEVs with uncontrolled charging (Base case, Approach 1, and Approach 2) are shown in Fig. 9. All charging stations have the same trend regardless of the number of WTGS that connected to the distribution system. With respect to this figure, the PEV batteries are fast filled, nevertheless, they still in the station for twelve hours.

Fig. 10 illustrates the SOC of PEVs of the charging station connected to bus 33 with optimal charging/discharging technique for 1 WTGS, 2 WTGS, and 3 WTGS. It can be noted that each PEV can charge/discharge based on its SOC and departure time to minimize the energy losses. Moreover, at the departure time, the SOC of the PEV is sufficient for driving (more than 65% at the departure time). Also, the planning problem has considered the PEVs previous day that arrive at the day end since they intend to persist charging/discharging at the starting of the studied day. Regarding the other charging stations that are connected to buses 36, 52, and 65, the SOC of PEVs connected at these stations have different trends of SOC than that of the charging station at buss 33, but they satisfy the required SOC at the departure time. From these results, we can note that considering the PEVs with the optimal charging control in the planning model for optimal allocation of WTGS can greatly reduce the annual energy losses in the distribution system while keeping enough SOC for each PEVs at departure time.

B. WTGS Allocation with enabled DSTATCOM Functionality

Here, the presented approach (Approach 3) is executed considering the DSTATCOM functionality of the interfacing inverter for determining the optimal allocation of the WTGS.

The results of Approach 3 considering the DSTATCOM functionality of the interfacing inverters of WTGS are shown in Table II. With respect to this table, we can observe that the locations of the WTGS are like those in Table I (Approach 3), but the capacities of WTGS are little different. Compared to the Base case, the energy losses are obviously decreased by employing the DSTATCOM functionality of the interfacing inverters. The annual energy loss reduction in the case of 1 WTGS, 2 WTGS, and 3 WTGS are 82%, 87%, and 88% respectively. Furthermore, by comparing Approach 3 in Table I with Table II, it can be observed that the consideration of DSTATCOM feature of the inverters yields a higher energy loss reduction. The hourly reactive powers of the interfacing inverters and average active power output in the case of 1 WTGS, 2 WTGS, and 3 WTGS are given in Figs. 11 and 12, respectively. It worth mentioning that by allocating 2 WTGS and 3 WTGS, there is no big difference in energy loss reduction. This means that the increase of WTGS numbers more than 3 has no further effect on energy loss reduction. For

TABLE II
RESULTS OF APPROACH 3 CONSIDERING DSTATCOM FUNCTIONALITY

Number of WTGS	Optimal bus	Number of WT units	Energy losses (MWh)	Energy loss reduction (%)
1 WTGS	61	13	312	82
2 WTGS	11	6	225	87
	61	13		
3 WTGS	11	4	203	88
	18	3		
	61	12		

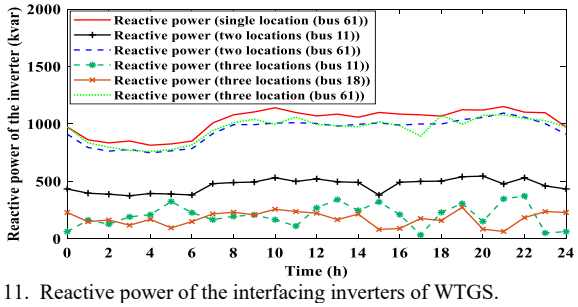

Fig. 11. Reactive power of the interfacing inverters of WTGS.

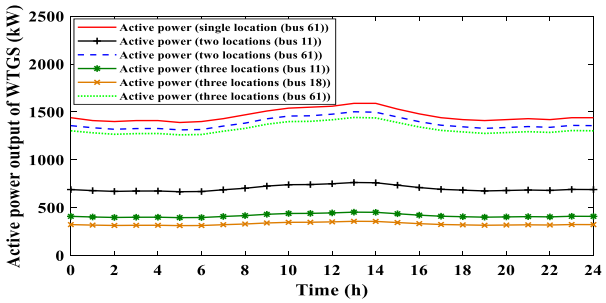

Fig. 12. Active power output of WTGS.

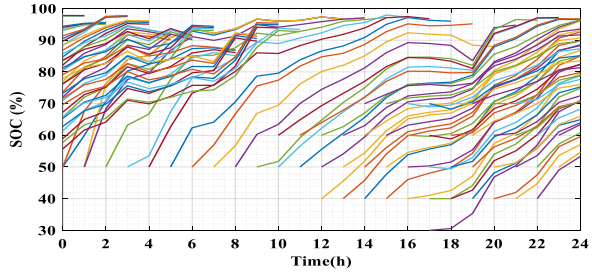

Fig. 13. SOC of PEV batteries with optimal charging/discharging scheme considering DSTATCOM functionality (3 WTGS).

instance, the energy loss reduction value with 2 WTGSs is 87 % which is almost equal to that with 3 WTGSs (88 %).

Fig. 13 shows the SOC of the PEVs in the case of allocating 3 WTGS in the distribution system considering DSTATCOM functionality of the interfacing inverters. Compared to Fig. 10 (c), the SOC values at departure time in Fig. 13 are higher than those in Fig. 10 (c). Therefore, the consideration of DSTATCOM functionality has positive impacts on the SOC of PEVS.

C. Impacts of Inverter oversizing on WTGS allocation

During high power generation from WTGS, the interfacing inverter is often fully loaded. To allow further reactive power capability, oversizing the interfacing inverters is a solution. For example, the IEEE 1547 standard suggests oversizing the interfacing inverter with 10% of its rated capacity [42]. By oversizing the inverter with 10%, the further reactive power capability will be about 46% of its rated capacity. In this subsection, we have allocated 3 WTGS by applying the proposed approach considering DSTATCOM functionality of oversized inverters by 10%. The results of this case are given in Table III. We can note that by allowing further reactive power capability of the interfacing inverters, the annual energy losses are greatly decreased compared to the Base case and Approach 3 in Tables I and II.

D. WTGS Allocation without PEVs and DSTATCOM Functionality

Here, we demonstrate the further benefits that can be accomplished by the consideration of PEVs and the DSTATCOM functionality of the interfacing inverter in the planning problem. To do so, we show the allocation results attained by a conventional approach [14], [43] that allocates WTGS without considering PEVs while the DSTATCOM functionality of the interfacing inverter is disabled. The results of this conventional approach for allocating 3 WTGS are listed in Table IV. By comparison of these results with the results of the proposed approach in Tables II and III, the efficiency and

TABLE III
RESULTS OF APPROACH 3 CONSIDERING DSTATCOM FUNCTIONALITY OF OVERSIZED INVERTERS

Number of WTGS	Optimal bus	Number of WT units	Energy losses (MWh)	Energy loss reduction (%)
3 WTGS	11	4	156	91
	18	3		
	61	12		

TABLE IV
RESULTS OF THE CONVENTIONAL APPROACH WITHOUT CONSIDERING PEVS AND DSTATCOM FUNCTIONALITY

Number of WTGS	Optimal bus	Number of WT units	Energy losses (MWh)	Energy loss reduction (%)
3 WTGS	11	4	682	60
	17	3		
	64	11		

superiority of the proposed approach over the conventional approach in minimizing the annual energy losses can be demonstrated. For example, the value of energy loss reduction is only 60% for the conventional approach while it has a much higher value of 91% by applying the proposed approach. This implies that considering the DSTATCOM functionality of the interfacing inverter and PEVs in the planning model can significantly decrease the annual energy losses.

VII. CONCLUSIONS

A bi-level optimization-based approach has been proposed in this paper for the optimal allocation of uncertain WTGS in the presence of PEVs. The proposed approach minimizes the energy losses, considers system constraints while complying with DSTATCOM functionalities of WTGS and the requirements of existing PEV infrastructures. A bi-level GWO algorithm has been proposed to accurately solve the comprehensive uncertain planning model. The upper and lower levels determine, respectively, the accurate WTGS allocation solution and the optimal PEV charging scheme in a simultaneous way. In particular, the lower level addresses the realistic operational requirement of PEVs, including initial and preset conditions of their state of charge, arriving and departing times, variously controlled and uncontrolled charging schemes. Various simulations on the 69-bus distribution system have been presented to demonstrate the effectiveness of the proposed approach. The charging scheme of PEVs and the inverter size of WTGS have resulted in considerable impacts on specifying the optimal capacities and locations of WTGS in distribution systems as well as minimizing the energy losses. The proposed approach is a helpful tool to be used by the system planners of distribution utilities for optimizing/quantifying future WTGS integration plans in the distribution system with PEVs.

REFERENCES

[1] M. A. Soliman, H. M. Hasanien, H. Z. Azazi, E. E. El-Kholy, and S. A. Mahmoud, "An Adaptive Fuzzy Logic Control Strategy for Performance Enhancement of a Grid-Connected PMSG-Based Wind Turbine," *IEEE Trans. Ind. Informatics*, vol. 15, no. 6, pp. 3163–3173, Jun. 2019.

[2] P. Lamaina, D. Sarno, P. Siano, A. Zakariazadeh, and R. Romano, "A Model for Wind Turbines Placement Within a Distribution Network Acquisition Market," *IEEE Trans. Ind. Informatics*, vol. 11, no. 1, pp. 210–219, Feb. 2015.

[3] M. Aly, E. M. Ahmed, and M. Shoyama, "Thermal and Reliability

Assessment for Wind Energy Systems With DSTATCOM Functionality in Resilient Microgrids," *IEEE Trans. Sustain. Energy*, vol. 8, no. 3, pp. 953–965, Jul. 2017.

[4] L. Lu, F. Wen, G. Ledwich, and J. Huang, "Unit commitment in power systems with plug-in hybrid electric vehicles," *Int. Trans. Electr. Energy Syst.*, vol. 23, no. 7, pp. 1205–1220, Oct. 2013.

[5] A. Ali, D. Raisz, K. Mahmoud, and M. Lehtonen, "Optimal Placement and Sizing of Uncertain PVs Considering Stochastic Nature of PEVs," *IEEE Trans. Sustain. Energy*, pp. 1–1, 2019.

[6] H. Nafisi, H. Askarian Abyaneh, and M. Abedi, "Energy loss minimization using PHEVs as distributed active and reactive power resources: a convex quadratic local optimal solution," *Int. Trans. Electr. Energy Syst.*, vol. 26, no. 6, pp. 1287–1302, Jun. 2016.

[7] E. A. M. Association and others, "A Review of Battery Technologies for Automotive Applications," *Eur. Automob. Manuf. Assoc. Brussels, Belgium*, 2014.

[8] C. H. Dharmakeerthi, N. Mithulananthan, and T. K. Saha, "A comprehensive planning framework for electric vehicle charging infrastructure deployment in the power grid with enhanced voltage stability," *Int. Trans. Electr. Energy Syst.*, vol. 25, no. 6, pp. 1022–1040, Jun. 2015.

[9] R. D'hulst, F. De Ridder, B. Claessens, L. Knapen, and D. Janssens, "Decentralized coordinated charging of electric vehicles considering locational and temporal flexibility," *Int. Trans. Electr. Energy Syst.*, vol. 25, no. 10, pp. 2562–2575, Oct. 2015.

[10] S. Xu, H. Pourbabak, and W. Su, "Distributed cooperative control for economic operation of multiple plug-in electric vehicle parking decks," *Int. Trans. Electr. Energy Syst.*, p. e2348, 2017.

[11] N. G. Paterakis and M. Gibescu, "A methodology to generate power profiles of electric vehicle parking lots under different operational strategies," *Appl. Energy*, vol. 173, pp. 111–123, Jul. 2016.

[12] N. Neyestani, M. Y. Damavandi, M. Shafie-Khah, J. Contreras, and J. P. S. Catalao, "Allocation of Plug-In Vehicles' Parking Lots in Distribution Systems Considering Network-Constrained Objectives," *IEEE Trans. Power Syst.*, vol. 30, no. 5, pp. 2643–2656, Sep. 2015.

[13] M. Mohammadi Landi, M. Mohammadi, and M. Rastegar, "Simultaneous determination of optimal capacity and charging profile of plug-in electric vehicle parking lots in distribution systems," *Energy*, vol. 158, pp. 504–511, Sep. 2018.

[14] Y. M. Atwa, E. F. El-Saadany, M. M. A. Salama, and R. Seethapathy, "Optimal Renewable Resources Mix for Distribution System Energy Loss Minimization," *IEEE Trans. Power Syst.*, vol. 25, no. 1, pp. 360–370, 2010.

[15] D. Q. Hung and N. Mithulananthan, "Multiple Distributed Generator Placement in Primary Distribution Networks for Loss Reduction," *IEEE Trans. Ind. Electron.*, vol. 60, no. 4, pp. 1700–1708, Apr. 2013.

[16] M. Vatani, G. B. Gharehpetian, M. J. Sanjari, and D. Solati Alkaran, "Multiple distributed generation units allocation in distribution network for loss reduction based on a combination of analytical and genetic algorithm methods," *IET Gener. Transm. Distrib.*, vol. 10, no. 1, pp. 66–72, Jan. 2016.

[17] K. Mahmoud, N. Yorino, and A. Ahmed, "Optimal Distributed Generation Allocation in Distribution Systems for Loss Minimization," *IEEE Trans. Power Syst.*, vol. 31, no. 2, pp. 960–969, 2016.

[18] V. Vahidinasab, "Optimal distributed energy resources planning in a competitive electricity market: Multiobjective optimization and probabilistic design," *Renew. Energy*, vol. 66, pp. 354–363, Jun. 2014.

[19] Y. Yi, Z. Zhang, D. Chen, R. Zhou, E. Patelli, and S. Tolo, "State feedback predictive control for nonlinear hydro-turbine governing system," *JVC/Journal Vib. Control*, vol. 24, no. 21, pp. 4945–4959, Nov. 2018.

[20] Y. Yi, D. Chen, and Q. Xie, "Controllability of nonlinear fractional order integrodifferential system with input delay," *Math. Methods Appl. Sci.*, vol. 42, no. 11, pp. 3799–3817, Jul. 2019.

[21] Y. Yi and D. Chen, "Disturbance observer-based backstepping sliding mode fault-tolerant control for the hydro-turbine governing system with dead-zone input," *ISA Trans.*, vol. 88, pp. 127–141, May 2019.

[22] H. Bagheri Tolabi, M. H. Ali, and M. Rizwan, "Simultaneous Reconfiguration, Optimal Placement of DSTATCOM, and Photovoltaic Array in a Distribution System Based on Fuzzy-ACO Approach," *IEEE Trans. Sustain. Energy*, vol. 6, no. 1, pp. 210–218, Jan. 2015.

[23] S. Ganguly and D. Samajpati, "Distributed Generation Allocation on Radial Distribution Networks Under Uncertainties of Load and Generation Using Genetic Algorithm," *IEEE Trans. Sustain. Energy*, vol. 6, no. 3, pp. 688–697, Jul. 2015.

[24] J. Mitra, M. R. Vallem, and C. Singh, "Optimal Deployment of Distributed Generation Using a Reliability Criterion," *IEEE Trans. Ind. Appl.*, vol. 52, no. 3, pp. 1989–1997, May 2016.

[25] B. R. Pereira, G. R. M. Martins da Costa, J. Contreras, and J. R. S. Mantovani, "Optimal Distributed Generation and Reactive Power Allocation in Electrical Distribution Systems," *IEEE Trans. Sustain. Energy*, vol. 7, no. 3, pp. 975–984, Jul. 2016.

[26] K. Seddig, P. Jochem, and W. Fichtner, "Integrating renewable energy sources by electric vehicle fleets under uncertainty," *Energy*, vol. 141, pp. 2145–2153, Dec. 2017.

[27] K. Qian, C. Zhou, M. Allan, and Y. Yuan, "Modeling of load demand due to EV battery charging in distribution systems," *IEEE Trans. Power Syst.*, vol. 26, no. 2, pp. 802–810, 2011.

[28] A. Ali, D. Raisz, and K. Mahmoud, "Optimal oversizing of utility-owned renewable DG inverter for voltage rise prevention in MV distribution systems," *Int. J. Electr. Power Energy Syst.*, vol. 105, pp. 500–513, Feb. 2019.

[29] Y. M. Atwa and E. F. El-Saadany, "Probabilistic approach for optimal allocation of wind-based distributed generation in distribution systems," *IET Renew. Power Gener.*, vol. 5, no. 1, p. 79, 2011.

[30] F. Samadi Gazijahani and J. Salehi, "Optimal Bilevel Model for Stochastic Risk-Based Planning of Microgrids under Uncertainty," *IEEE Trans. Ind. Informatics*, vol. 14, no. 7, pp. 3054–3064, 2018.

[31] A. R. Abul'Wafa, "Optimization of economic/emission load dispatch for hybrid generating systems using controlled Elitist NSGA-II," *Electr. Power Syst. Res.*, vol. 105, pp. 142–151, 2013.

[32] S. H. Jangamshetti and V. G. Rau, "Site matching of wind turbine generators: a case study," *IEEE Trans. Energy Convers.*, vol. 14, no. 4, pp. 1537–1543, 1999.

[33] Y. Zhang, K. Meng, F. Luo, Z. Y. Dong, K. P. Wong, and Y. Zheng, "Optimal allocation of battery energy storage systems in distribution networks with high wind power penetration," *IET Renew. Power Gener.*, vol. 10, no. 8, pp. 1105–1113, Sep. 2016.

[34] "Hummer H25.0-200KW - 200,00 kW - Wind turbine." [Online]. Available: https://en.wind-turbine-models.com/turbines/1681-hummer-h25.0-200kw?fbclid=IwAR2l3AJbCjbsce1MHQkyZNpsx14qAaIOa5uZIRZzBK84jkDXGq4kLm0jtQg. [Accessed: 28-Jan-2020].

[35] S. Mirjalili, S. M. Mirjalili, and A. Lewis, "Grey wolf optimizer," *Adv. Eng. Softw.*, vol. 69, pp. 46–61, 2014.

[36] U. Sultana, A. B. Khairuddin, A. S. Mokhtar, N. Zareen, and B. Sultana, "Grey wolf optimizer based placement and sizing of multiple distributed generation in the distribution system," *Energy*, vol. 111, pp. 525–536, 2016.

[37] M. E. Baran and F. F. Wu, "Network reconfiguration in distribution systems for loss reduction and load balancing," *IEEE Trans. Power Deliv.*, vol. 4, no. 2, pp. 1401–1407, Apr. 1989.

[38] X. Wu, X. Hu, S. Moura, X. Yin, and V. Pickert, "Stochastic control of smart home energy management with plug-in electric vehicle battery energy storage and photovoltaic array," *J. Power Sources*, vol. 333, pp. 203–212, 2016.

[39] S. Shafiee, M. Fotuhi-Firuzabad, and M. Rastegar, "Investigating the Impacts of Plug-in Hybrid Electric Vehicles on Power Distribution Systems," *IEEE Trans. Smart Grid*, vol. 4, no. 3, pp. 1351–1360, Sep. 2013.

[40] "Historical Climate Data - Climate - Environment and Climate Change Canada." [Online]. Available: http://climate.weather.gc.ca/. [Accessed: 28-Aug-2019].

[41] "European Network of Transmission System Operators for Electricity." [Online]. Available: https://www.entsoe.eu/. [Accessed: 28-Aug-2019].

[42] I. S. Association, "IEEE standard for interconnection and interoperability of distributed energy resources with associated electric power systems interfaces," *IEEE Std 1547-2018 (Revision IEEE Std 1547-2003)*, pp. 1–227, 2018.

[43] F. Alismail, P. Xiong, and C. Singh, "Optimal Wind Farm Allocation in Multi-Area Power Systems Using Distributionally Robust Optimization Approach," *IEEE Trans. Power Syst.*, vol. 33, no. 1, pp. 536–544, Jan. 2018.

Abdelfatah Ali was born in Egypt on October 19, 1986. He received the B.Sc. degree and the M.Sc. degree in electrical engineering from Aswan University, Aswan, Egypt, in 2009 and 2013, respectively. In 2019, he received the Ph.D. degree from the Doctoral School of Electrical Engineering, Faculty of Electrical Engineering and informatics, Budapest University of Technology and Economics, Budapest, Hungary. Since 2010, he has been an Assistant Lecturer with the Faculty of Engineering, South Valley University (SVU), Qena, Egypt. He is currently working as an Assistant Professor with SVU. His research interests include modeling, analysis, control, and optimization of distribution systems with distributed generation and electric vehicles.

Karar Mahmoud received the B.S. and M.Sc. degrees in electrical engineering from Aswan University, Aswan, Egypt, in 2008 and 2012, respectively. In 2016, he received the Ph.D. degree from the Electric Power and Energy System Laboratory (EPESL), Graduate School of Engineering, Hiroshima University, Hiroshima, Japan. Since 2010, he has been with Aswan University where he is presently Assistant Professor. Currently, he is a Postdoctoral Researcher at the School of Electrical Engineering, Aalto University, Finland. His research interests include Power Systems, Renewable Energy Sources, Smart Grids, Distributed Generation, and Optimization.

David Raisz (M'06–SM'18) received the M.Sc. degree and the Ph.D. degree in electrical engineering from the Budapest University of Technology and Economics (BUTE), Budapest, Hungary, in 2000 and 2011, respectively. From 1999 to 2001, he joined the Graz University of Technology, Austria, as a Guest Researcher. From 2012 to 2016, he led the Power Systems and Environment Group with the Department of Electric Power Engineering, BUTE, as an Associate Professor. In 2017, he joined the Institute for Automation of Complex Power Systems within the E.ON Energy Research Center, RWTH Aachen University. He has been working on or leading more than 40 industrial and research projects.

Matti Lehtonen received the M.Sc. and Licentiate degrees in electrical engineering from the School of Electrical Engineering, Aalto University (formerly Helsinki University of Technology), Espoo, Finland, in 1984 and 1989, respectively, and the D.Sc. degree from the Tampere University of Technology, Tampere, Finland, in 1992. Since 1987, he has been with VTT Energy, Espoo, and since 1999, he has been with the School of Electrical Engineering, Aalto University, where he is currently the Head of Power Systems and High Voltage Engineering Department. His main activities include earth fault problems, and harmonic related issues and applications of information technology in distribution automation and distribution energy management.